ORIGINAL ARTICLE

Anti-atherosclerotic activity of Betulinic acid loaded polyvinyl alcohol/methylacrylate grafted Lignin polymer in high fat diet induced atherosclerosis model rats

Juan Zhang [a], **Hesham S. Almoallim** [b], **Sulaiman Ali Alharbi** [c], **Baihui Yang** [d],*

[a] *Department of Internal Medicine-Cardiovascular, The Second Affiliated Hospital of Zhengzhou University, Zhengzhou City, Henan Province 450014, China*
[b] *Department of Oral and Maxillofacial Surgery, College of Dentistry, King Saud University, P.O. Box-60169, Riyadh 11545, Saudi Arabia*
[c] *Department of Botany and Microbiology, College of Science, King Saud University, PO Box-2455, Riyadh 11451, Saudi Arabia*
[d] *Department of Cardiovascular Surgery, The Second Affiliated Hospital of Kunming Medical University, Kunming, Yunnan 650101, China*

Abstract Betulinic acid is one such natural pentacyclic triterpenoid compound, holding various pharmacological properties but its poor bioavailability is the only limitation. One of the biological macromolecules such as Lignin is a plant-derived aromatic, eco-friendly and low-cost polymer that certainly self-assembles into nano-sized colloids. Therefore, onto the current investigation, we increased the bioavailability of betulinic acid by coating on to a nanopolymer prepared with poly vinyl alcohol, lignins and methyl acrylate. Betulinic acid loaded polyvinyl alcohol/ethylacrylate grafted Lignin polymer (PVA/Lig-g-MA) nanoformulation was characterized using FTIR, XRD, SEM and TEM analysis and also the drug entrapment, *in vitro* drug releasing capacity was done to examine the efficiency of the nanoformulation of a drug. The MTT assay was evaluated the cytotoxicity of synthesized nanoformulation against normal endothelial cells HUVEC and HAPEC to confirm the side effects of the drug. The anti-atherosclerotic property of the nanoformulation was ascertained in both *in vitro* condition (with HUVEC and HPAEC) and *in vivo* studies (with Wistar rats). As a result, the characterization studies and *in vitro* studies clearly confirmed the Betulinic

* Corresponding author at: Department of Cardiovascular Surgery, The Second Affiliated Hospital of Kunming Medical University, Kunming, Yunnan 650101, China.
E-mail address: kmyangbh@sina.com (B. Yang).

acid loaded PVA/Lig-g-MA nanoformulation is an ideal nanopolymer and it doesn't cause any cytotoxic effect in normal endothelial cells. It also decreased the lipopolysaccharides induced inflammation through the down-regulation of NFκB and MAP/JNK signaling molecule expressions. Following *in vivo* results confirmed the synthesized nanoformulation effectively decreased the hyperchlostremia, inflammation and vasoconstriction, which induced over high fat diet. The results of histopathological analysis of cardiac tissues also confirmed the cardioprotective role of synthesized nanoformulation. Overall, both the *in vitro* and *in vivo* studies authentically proven the Betulinic acid loaded PVA/Lig-g-MA nanoformulation would be a potent cost effective anti-atherosclerotic nanodrug.

1. Introduction

Globally, the growing of cardiovascular diseases (CVD) is a serious health concern of both developed and developing countries, which roughly accounting death of about 31%. In developing countries like USA, the death rate by CVD has been drastically increased from 18.6% to 31.8% in ten years (Benjamin et al., 2019). The pathological condition of atherosclerosis is a main inducer of CVD, which is characterized by lipid accumulation in coronary arteries leading to plaque formation and arterial endothelial cells dysfunction. Besides, there are so many risk factors involved in the development of atherosclerosis including high cholesterol level, hypertension, obesity, smoking, alcohol consumption, genetic susceptibility, gender, race etc. (McLaren et al., 2011). Inflammation is a crucial function to initiate endothelial dysfunction for the development of atherosclerosis plaque in coronary arteries (Wang and Nakayama, 2010).

Hyperchlosteremic condition associated with CVD was reported in most of the patients that primarily induced inflammatory atherosclerotic lesions and following cause decreased blood turbulence and finally leading to stroke (Subramani et al., 2017). Therefore, most of the drug prescribed for CVD is lipid lowering drugs and anti-inflammatory drugs such as statins, ezetimibe, colesevelam, niacin etc. Even though it's effective for CVD treatment, the causing of side effects are also not negotiable (Pahan, 2006). Therefore, it a global need to discover powerful as well as no side effects treatment. Herbal based drugs are boon for mankind than allopathic drugs because of its potential ingredients. One such herbal compound is Betulinic acid (BA), a pentacyclic triterpenoid compounds present in the bark of the white birch (*Betula pubescens*) possessing numerous pharmacological actions like anti-inflammatory, antitumor, anti-bacterial, anti-viral, antiatherosclerotic, antidiabetic etc. (Takada and Aggarwal, 2003; Yogeeswari and Sriram, 2005; Mathew et al., 2017). Since its effectively decreases the blood cholesterol, it is used to treat obesity (de Melo et al., 2009). But, the major drawback of this betulinic acid has its poor solubility in aqueous solution and its reduced bioavailability. Hence the present study, we formulated the betulinic acid into a nanodrug to treat atherosclerosis effectively (Godugu et al., 2014; Harwansh et al., 2017).

Electro spinning is a unique easy and flexible method to make polymer nanofibrous materials (Nayani et al., 2012). Electrospun materials have various attractive properties like high specific surface to volume ratio, high porosity, great mechanical properties, homogeneous morphology to natural extracellular matrix (ECM) and easy preparation methods at micro to nano scales from wide natural and synthetic polymers (Safaee-Ardakani et al., 2019; Sadri et al., 2015). Although, the polymer nanofibers prepared by electrospinning method are not strong as expected particularly in very small diameters and unoptimized molecular direction. Stretching and prepared polymer composites can improve the mechanical properties of polymeric nanofiber (Kadavil et al., 2019; José, 2008).

Various types of natural and synthetic polymers are used on electrospun nanofiber preparation such as natural polymer like chitosan (Faralli et al., 2019), gelation (Heidari et al., 2019) and silk (Kalani et al., 2019) etc., synthetic polymer like poly ethylene glycol (PEG) (Hobzova et al., 2019), poly caprolactone (PCL) (Ma et al., 2019), poly lactic acid (PLA) (Gu et al., 2019) and poly vinyl alcohol (PVA) (Xiao et al., 2019) PVA is a non-toxic, hydrophilic, biocompatible and biodegradable materials and widely used in biomedical applications (Jatoi et al., 2019). Lignin macromolecules is a plant-derived aromatic polymer, mainly made up of phenolic derivatives known as monolignols (Huang et al., 2019; Huang et al., 2018). Lignin macromolecules is eco-friendly and low-cost polymer that certainly self-assembles into nano-sized particles/colloids (Figueiredo et al., 2018). Lignin macromolecules is primarily derived as a by-product in pulp industries from alkaline kraft processes. Other sources of lignin are ethanol production and various lignocellulosic biomass pre-treatment techniques (Santos et al., 2017; Martín-Sampedro et al., 2019). The significant efforts have been devoted to upgrade lignin to high-value chemicals (Guo et al., 2013; Yang and Wyman, 2008). The various inter-molecular connections, molecular weight distributions, and chemical reactions that originates from the different lignin separation methods and diverse plant origins are leads to challenges that in need to be resolved (Vishtal and Kraslawski, 2011; Welker et al., 2015). As following, Methyl Acrylate (MA) is another hydrophilic, pH-sensitive and biocompatible synthetic polymer utilized in numerous biomedical applications (Huang et al., 2018). Therefore, we formulated a nanodrug with PVA, lignins, MA coated with herbal compound betulinic acid and assessed its antiatherosclerotic activity in *in vitro* and *in vivo* conditions.

2. Materials and methods

Lignin sulphonic acid sodium salt, methylacylate, ammonium persulfate (APS), polyvinyl alcohol (PVA), dimethyl sulfoxide

(DMSO) was acquired from Himedia, USA. The Betulinic acid was obtained from Sigma Aldrich, St. Louis, USA. All the solvents and reagents were utilized for further purification. Finally DD water was used throughout the experiment section.

2.1. Synthesis of methylacrylate grafted Lignin polymer (Lig-g-MA)

Lig-g-MA polymer was already reported our previous work via graft copolymerization of MA and Lig polymer APS used as a free radical initiator (Figueiredo et al., 2018). In brief, 6 mL of MA was poured into the 100 mL of three-necked RB flask which contained Lignin water solution (8 mg/4 mL). Then, APS (100 mg) was suspended in 10.0 mL distilled water. The whole setup was carried out at thermostated water bath at 80 °C for 3 h under N_2 atmosphere. Then, APS solution was mixed slowly into MA contained Lignin solution. Further, the polymer was chilled to room temperature and put into 50 mL of ethanol solution to remove the unreacted Lignin. Finally, Lig-g-MA was completely settled down. Then the polymer was separated and dehydrated at ambient room temperature for 24 h.

2.2. Synthesis of polyvinyl alcohol/methylacrylate grafted Lignin polymer (PVA/Lig-g-MA)

The 80 mg of PVA solution was prepared by dissolving PVA into DMSO (6 mL) on stirring for 24 h stirring at room temperature. Simultaneously, the Lig-g-MA solution was prepared at a concentration of 20 mg polymer, which was suspended in 3 mL of DMSO under constant stirring at 37 °C for 24 h. Then, the Lig-g-MA polymer solution was mixed to PVA solution and again stirring for another 24 h under ambient room temperature. At last, the homogeneous mixture solution of PVA/Lig-g-MA with a total volume ratio of 80:20 was obtained.

2.3. Electrospinning process

The prepared electrospinning blending polymer solutions were poured into 2 mL of syringe that was connected to a needle gauge size of (0.55 × 25 mm/24 × 1). Then the needle filled with polymer solution was placed under high voltage of 16 kV, supplied by high voltage introducer. And the flowing rate of the solution at 0.5 mL/h was controlled by syringe ump that applied for the electrospinning process. The distance between the spinnerets and drum collected was 20 cm. At normal room temperature (27 °C), the fibers were collected from aluminium foil that covered drum collector. Eventually, the obtained nanofibers were dried under hot air oven for 24 h to remove the residual solvents (Santos et al., 2017).

2.4. Determination of encapsulation efficiency and loading capacity

First, 250 mg of PVA/Lig-g-MA polymer was dissolved in 4.5 mL of DMSO under room temperature for 5 h and then 10 mg/mL drug was dissolved in DMSO. Following this, the drug solution was gradually mixed to polymer solution and kept in stirrer for 12 h at ambient temperature to attain a uniform drug loaded solution. The encapsulation efficiency and loading capacity of betulinic acid was measured by UV–visible spectrometer at λ_{max} value of 210 nm.

$$EM(\%) = \frac{\text{Total amount of drug} - \text{Free amount of drug}}{\text{Total amount of drug}} \times 100$$

(1)

2.5. In-vitro drug release studies

At 37 °C, the in-vitro drug release profiles of betulinic acid from PVA/Lig-g-MA nanofibers were studied in different pH conditions such as 2.8 and 6.8. Selectively, 10 mg of drug loaded nanofibers was put into dialysis membrane (MW cut off 12,000) and the dialysis membrane was poured into 20 mL of PBS solution with two different pHs i.e. 2.8 and 6.8. The solution of nanofibers suspensions was placed into a magnetic stirrer at 150 rpm conditions. A 2 mL of releasing solution was taken out from the releasing medium at preferred time intervals and added an equal amount freshly prepared PBS solution in to that to determine the releasing amount of betulinic acid. This in-vitro release was measured by UV–visible spectrometer at λ_{max} value of 205 nm.

2.6. Characterization studies

Chemical structural functionalization of as prepared fiber mats were characterized by Fourier-transform infrared spectroscopy (FT-IR) (spectrum GX-1, Perkin Elmer and USA) at a wave number range of 4000 cm^{-1} to 400 cm^{-1}. The surface morphology of prepared fiber mats was evaluated by using scanning electron microscope (VEGA3SB, TESCAN and Czech), the fiber mats were placed on carbon tab coated aluminum grid to allow sputter for 15 min and the images were captured by SEM microscopy. Another advanced surface morphology analyzer HR-TEM (model Tecnai Philips F30, FEI Co., Hillsboro) was also used. The crystal phase of the synthesis fiber mats were analyzed by using Philips 1710 X-ray diffractometer (Philipps Electronic Instruments, Inc., Mahwah, NJ). The drug encapsulation, loading capacity and in-vitro drug release profile of fibers were determined via UV–vis spectrophotometer (Shimadzu-1600, Japan).

2.7. In vitro atherosclerotic model

2.7.1. Culturing of cells

Two types of normal endothelial cells were used. First, the Human Umbilical Vein Endothelial Cells (HUVEC) was opted as in vitro model for angiogenesis, which isolated from the umbilical tissue. Secondly, Human Pulmonary Artery Endothelial Cells (HPAEC) was preferred as a model of atherosclerosis that isolated from pulmonary tissue to detect the cytotoxicity potential of synthesized nanoformulation. Both the cell lines were procured from Sigma Aldrich, USA and were cultured with endothelial cell growth medium consisting of the supplements like growth factors. The cells were maintained at 37 °C with 5% CO_2 for a period of 72 h. The medium was changed for every 48 h upon obtaining 80% confluence, where the cells were subcultured using Trypsin-EDTA solution for further experiments.

2.7.2. Cytotoxicity assay

The cytotoxicity of synthesized nanoformulation Betulinic acid loaded PVA/Lig-g-MA was assessed using MTT assay in 24 well sterile culture plates, where 0.05×10^6 cells were seeded to the plate and incubated at 37 °C with 5% CO_2. The cells were then supplemented with one set doses (0–40 μg/ml) of nanoformulation synthesized and rest of the cells were supplemented with another set doses (0–10 μg/ml) of lipopolysaccharides obtained from Sigma Aldrich, USA and incubated at 37 °C with 5% CO_2 for 24 h. The cells were treated with lipopolysaccharides to compare the results obtained from the cells treated with nanoformulation. After incubation period, the culture medium was discarded and 20 μl of MTT was dropped to every well and incubated for 4 h at 37 °C with 5% CO_2. By adding 150 μl of DMSO, the MTT acquired formazon crystals were suspended and their optical density was measured at 560 nm using the microplate reader. The experiment was repeated thrice and the viability of cells was calculated using following formula:

$$\text{Cell viability } (\%) = \frac{\text{OD of test sample}}{\text{OD of control sample}} \times 100\%$$

2.7.3. Nitrite assay

Nitrate-Nitrite-Nitric Oxide pathway critically determines the inhibition or activation of an inflammatory reaction. Therefore in the present study, we estimated the inhibition of nitrite synthesis by Betulinic acid loaded PVA/Lig-g-MA nanoformulation. First, the cells were treated with 10 μg/ml of LPS to induce the generation of nitrite and the cells were subsequently supplied with diverse dosages (0–40 μg/ml) of Betulinic acid loaded PVA/Lig-g-MA nanoformulation and at last simvastin, standard drug treated cells were kept as positive control. Then the cells were incubated for 24 h at 37 °C with 5% CO_2 to estimate the nitrite concentration using Nitrite Assay kit, BioVision. Again, the cells were incubated Griess reagent A, B and nitrite Assay buffer for 10 min at room temperature. After that, the intensity of color developed was measured at 540 nm using microplate reader. The amount of nitrite was illustrated as standard curve drawn with values of different concentration of standard samples.

2.7.4. Prostaglandin E2 assay

Synthesize of Prostaglandin E2 (PGE2) from Prostaglandin H2 acts as both proinflammatory as well as anti-inflammatory agents. For nitrite assay, the same treatment procedures were followed for both HUVEC and HPAEC cells. Then the treated cells were subjected to Prostaglandin E2 Assay via commercial ELISA kit, Abcam, USA. The normal and supplemented samples were mixed with alkaline phosphatase (AP) conjugated-Prostaglandin E2 antibody to pre-coat the ELISA plate and incubated at RT for 2 h. Then added p-nitrophenyl phosphate to the plate after washed thrice it with buffer and incubated for 45 min at RT. The reaction was quenched by adding stop solution and finally the intensity of the developed yellow color was examined at 405 nm.

2.7.5. Inflammatory cytokines assay

The inflammatory cytokines are broad range of low molecular weight proteins which act as both pro and antiatherogenic. We estimated the inflammatory cytokines TNFα, IL-6 and IL-1β via commercial ELISA kit (MyBiosource, USA). The treatment protocol for cells was similar as that of nitrite assay. The cells were assessed using Tumor necrosis factor α (MBS490377), Interleukin 6 (MBS490361), and Interleukin1β (MBS772107). The procedure was followed as per the manufacture's protocol and the readings were taken at 450 nm. The levels of cytokines were calculated by standard curve drawn with the standard values.

2.7.5.1. Cytoplasmic and nuclear fraction separation.

HUVEC cells were maintained to the same experimental protocol followed in immunoblotting analysis. The cells were subjected to cytoplasmic and nuclear fraction separation for better understanding of signaling molecules. After 24 h incubation with 10 μg/ml LPS and different concentration of nanoformulation. Then the cells harvested with trypsin-EDTA and cleaned with chilled phosphate buffer saline to separate the cytoplasmic and nuclear fractions. To extract the cytoplasmic fraction, the cells were suspended in the cytoplasmic extraction buffer containing 20 mM HEPES pH 7.9, 10 mM KCl,1 mM EDTA, 0.2% NP40, 10% Glycerol, 1 mM DTT along with protease and phosphatase cocktail inhibitor. Then it was centrifuged at 9800g for 2 min at 4 °C and the cytoplasmic fraction was found in the supernatant. The collected pellet were re-suspended by nuclear fraction extraction buffer which is same as cytoplasmic extraction buffer, which replaced 0.2% NP40 to 400 mM NaCl and 10% Glycerol to 20% Glycerol. Then the cells were incubated for 30 min at 4 °C and centrifuged at 9800g for 5 min. The collected supernatant contains nuclear fraction that was used for further analysis (Martín-Sampedro et al., 2019).

2.7.6. Immunoblotting analysis

Immunoblotting analysis analyzed NF- κ β and ERK pathway signaling protein in the control and nanoformulation treated cells. The obtained cytoplasmic and nuclear fractions were subjected to protein estimation using Bradford reagent. In every sample, 40 μg of protein were electrophoresed with SDS- Polyacrylamide gel at 100 mV for 2 h. The electrophoresed gel was then blotted on to PVDF membrane at 100 mV for 1 h and this membrane was incubated for 2 h with 5% skimmed milk blocking buffer on a rocking shaker at 37 °C to block the unspecific antibodies binding on to the membrane. This membrane was consecutively washed with PBS and incubated with primary monoclonal antibodies of NF-κB signaling proteins pIκB-α, IκB-α, pIκκB-α, IκκB-α, NF-κB/p65 and MAP/JNK signaling proteins ERK1/2, pERK1/2, pAKT, AKT, pJNK, JNK, p38, Pp38 for overnight at 4 °C. The membranes were then incubated for 1 h with HRP conjugated secondary antibodies and the specific protein bands were then visualized using Enzyme chemiLuminiscence kit (Millipore, USA) under ChemDoc scanner. The membranes were stripped using stripping and then again incubated with internal control protein β actin and laminin.

2.8. In vivo atherosclerotic model

2.8.1. Animals

Health young male Wistar rats (6–8 weeks) weighing about 200–220 g were procured from institution animal house. Before beginning of treatment, the rats were acclimatized for

a week in a standard laboratory condition of 24 ± 3 °C, 50–60% humidity with 12 h light/dark cycle. The rats were bedded daily with sterile paddy husk and the cages were changed three days once. The rats were fed ad libidum with standard rat pellet diet and reverse osmosis water. All experimental procedures executed were permitted by the institutional ethical committee (IAEC No: XQYY-LUNLI-FJ004.1213), The Second Affiliated Hospital of Air Force Medical University of People's Liberation Army, Xi'an, Shaanxi, China. The rats were treated with highest care and concern in every possible means to minimize the discomfort.
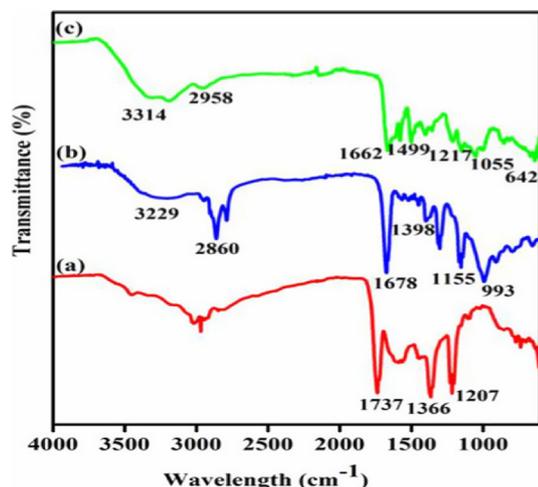
Fig. 1 Nanoformulation physical characterization. Fourier-transform infrared spectroscopy analysis of synthesized Betulinic acid loaded PVA/Lig-g-MA nanoformulation. FTIR spectrum of (a) Lig-g-MA, (b) PVA/Lig-g-MA and (c) Betulinic acid loaded PVA/Lig-g-MA nanofiber.

2.8.2. Experimental protocol

After acclimatization period, the rats were grouped randomly into five groups, each consists of 10 rats. Group-I rats were regarded as control rats that fed with standard diet, Group-II rats were atherosclerosis induced rats which were fed with high fat diet (D12451 Research Diets, New Brunswick, NJ, USA) for a period of 30 days. Group-III and IV rats were fed with high fat diet and simultaneously treated with low dose 25 mg/kg b.wt Betulinic acid loaded PVA/Lig-g-MA nanoformulation and high dose 50 mg/kg b.wt Betulinic acid loaded PVA/Lig-g-MA nanoformulation respectively. At last, the atherosclerosis induced Group V rats were considered as positive control rats which fed with high fat diet and simultaneously treated with simvastatin, a standard anti-atheroclerostic drug for a period of 30 days. The amount of food intake of each group of rats were measured and recorded daily. The weights of each rat were measured weekly once and the values were recorded to analyze the induction of obesity caused by high fat diet.

2.8.3. Sample collection

After 24 h of experimental period, the rats were anesthetized using diethyl ether and the blood sample was collected via heart puncture with 5 mL syringe. The blood was immediately transferred to a sterile plain tube for the separation of serum. After euthanizing the rats with CO_2 gas, the heart tissue was excised carefully and it was stored at −80 °C for further analyses.

2.8.4. Lipid profile analysis

The blood samples collected were centrifuged at 5000 rpm for 5 min to separate the serum samples. The lipid profile, the total cholesterol, total glyceride, HDL cholesterol, LDL cholesterol and VLDL cholesterol were investigated via commercial enzymatic kits. The Cholesterol Assay Kit - HDL and LDL/VLDL
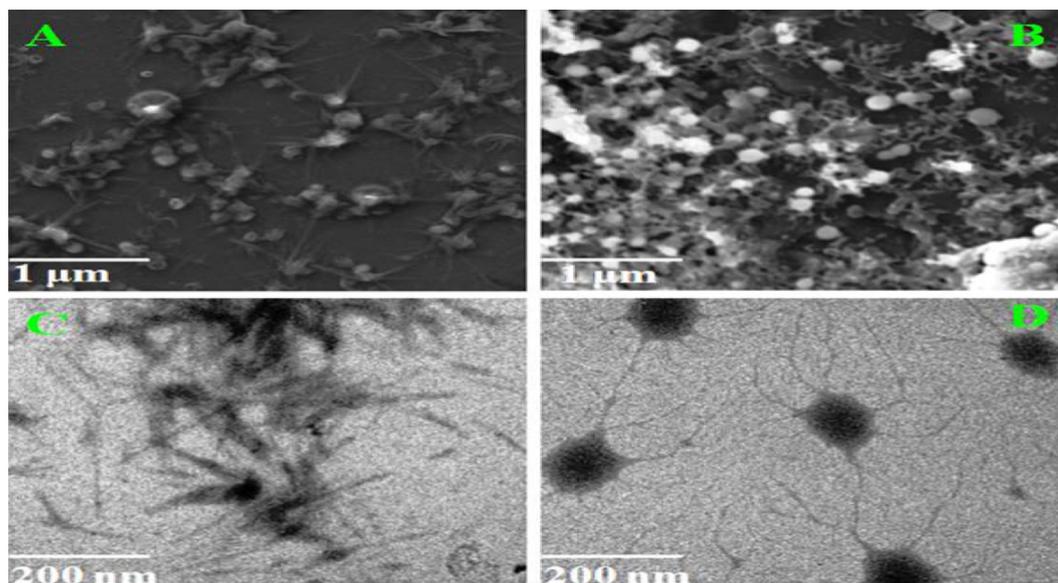
Fig. 2 Nanoformulation physical characterization. Electron Microscopic images of synthesized Betulinic acid loaded PVA/Lig-g-MA nanoformulation. *A&B-* SEM images of PVA/Lig-g-MA and Betulinic acid loaded PVA/Lig-g-MA and *C&D-* TEM images of PVA/Lig-g-MA and Betulinic acid loaded PVA/Lig-g-MA.

(ab65390) kit were procured from Abcam, USA. The assay was performed according to manufacturer guidelines and the whole serum was used for estimating total cholesterol. In order to detect the levels of HDL cholesterol, the sample was precipitated by incubating with precipitation buffer for 10 min and centrifuged at 2000g for 10 min. Also, the levels of LDL and VLDL cholesterol were measured using the following formula

$$LDL\left(\frac{mg}{dl}\right) = TC - HDL - TG/5$$

$$VLDL\left(\frac{mg}{dl}\right) = TG/5$$
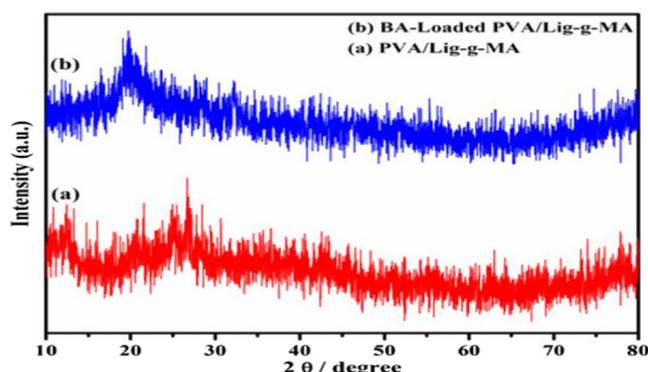
Fig. 3 Nanoformulation physical characterization. X-Ray Diffraction pattern analysis of synthesized Betulinic acid loaded PVA/Lig-g-MA nanoformulation.
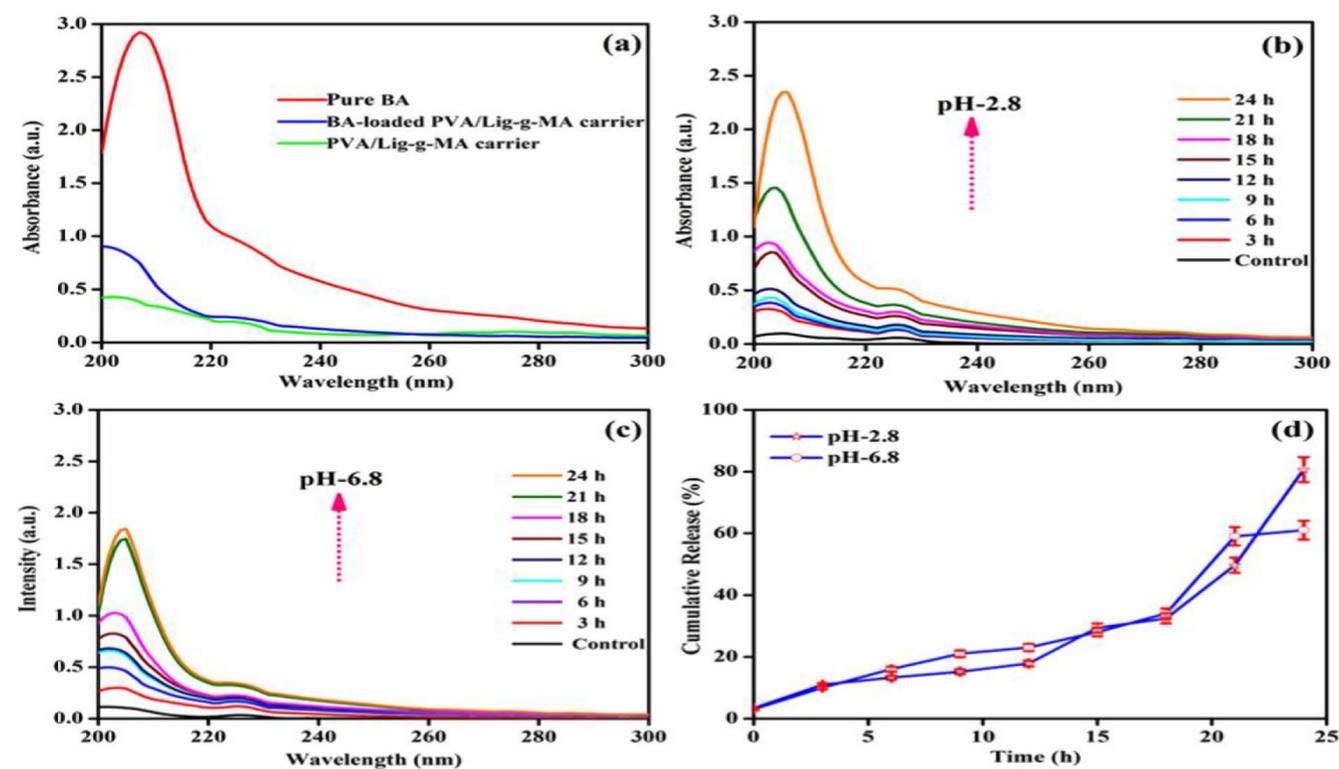
Eventually, the triglyceride (TG) levels were examined via commercial colorimetric Triglyceride Quantification Assay Kit (ab65336), Abcam, USA. The end point reaction was measured at OD 570 nm using microplate reader.

2.8.5. Inflammation and liver function analysis

The anti-inflammatory property and the effect of Betulinic acid loaded PVA/Lig-g-MA nanoformulation on the liver functioning in high fat diet rat model was quantified by estimating the levels of interleukins and liver function testing enzymes. The levels of interleukins were inspected via commercial ELISA assay kits IL-8 (ABIN2535650), IL-18 (ab213909), IL-1 beta (ab100768), C - reactive protein (ab108827), Abcam, UK. The tests were performed as per the manufacturer guidelines and the end results were measured at 450 nm using microplate reader.

The status of liver functioning enzymes was analyzed using commercial colorimetric kits of alanine transaminase (MAK052), aspartate transaminase (MAK055-1KT), alkaline phosphatase (ab83369) and lactate dehydrogenase (MAK066).

2.8.6. Vasodilators analysis

The induction of vasodilators by Betulinic acid loaded PVA/Lig-g-MA nanoformulation was estimated using commercially available kits of nitric oxide (ab65328), endothelin (ab133030), 6-keto-Prostaglandin F1α (ab133023). These assays were performed in accordance to the guidelines of the manufacturer.

2.8.7. Histopathological analysis

3–4 mm of heart tissue was expunged from normal and treated rats were fixed with 10% formalin for 2 days and then the

Fig. 4 In-vitro drug release studies of synthesized Betulinic acid loaded PVA/Lig-g-MA electrospun nanofiber under various pH-conditions. (a) Entrapment efficiency (b) pH-2.8 (c) pH-6.8 and (d) Cumulative drug release profiles.

samples were dehydrated with series of xylene and ethanol solutions. The dehydrated tissue was embedded in paraffin wax and then cut into thin sections of 5 μm. The sections were fixed on to the albumin coated slides and further subjected to hematoxylin and eosin staining. The stained slides were focused under the confocal microscope and the sections were photographed for further analysis.

3. Results and discussion

In this study, our findings from the physical characteristic analysis, *in vitro* drug releasing capacity of Betulinic acid loaded PVA/Lig-g-MA nanoformulation suggested that it would be an ideal drug to treat the atherosclerosis. The findings of *in vitro* studies, demonstrated that it effectively diminished the levels of lipids, interleukins and increased the levels of vasodilators thereby preventing the myocardial cells from degeneration. It was also evidenced the hepatoprotective effect of synthesized nanoformulation against high fat diet induced liver damage. One of the most chief causative agents of cardiovascular disease is an atherosclerotic plaque, the lipid foam accumulation on the walls of coronary arteries leading to blockade of blood vessels eventually causing CVD. Hyperlipidemia along with oxidative stress leads to inflammatory reaction thereby mediates the formation of atherosclerotic plaques (Guo et al., 2013). Betulinic acid, 3β-hydroxylup-

20(29)-en-28-oic acid, BA, (1), is a natural pentacyclic-tripenoids present in plants like Pulsatilla chinensis, *Quisqualis fructus, Coussarea paniculata, Tetracentron sinense, Uapaca nidid* etc. (Yogeeswari and Sriram, 2005). It possesses immense biological benefits like anti-inflammatory, anti-viral, antibacterial, antitumor and it is used as chemotherapeutic drug (Yang and Wyman, 2008; Vishtal and Kraslawski, 2011; Welker et al., 2015).

In the present study, we formulated a nanodrug by grafting lignin to methyl acrylate. Lignin is a natural and universal available biodegradable polymer formed by random cross linking of hydroxylated and methoxylated phenyl propane. Lignin imparts mechanical strength to the polymer drug and it also possess antioxidant, antimicrobial properties which thereby increases the efficacy of the nanodrug (Vinothini et al., 2019; Hussein-Al-Ali et al., 2014). Methyl acrylate increases the hydrophilic nature of the conjugated drug without producing any side effect on the drug. The addition of hydroxyl or carboxyl group to a polymer has been reported to increase the hydrophilic property of drug (Jeyaraj, 2016). Therefore, we grafted lignin with methylacrylate to synthesis a hydrophilic polymer and ultimately develop methylacrylate grafted lignin by adding polyvinyl alcohol.

Polyvinyl alcohol is a non-toxic biodegradable polymer widely used to increase the mechanical strength and hydrophilic nature of a compound (Santos et al., 2007). In order to enhance the hydrophilic property more, we linked polyvinyl
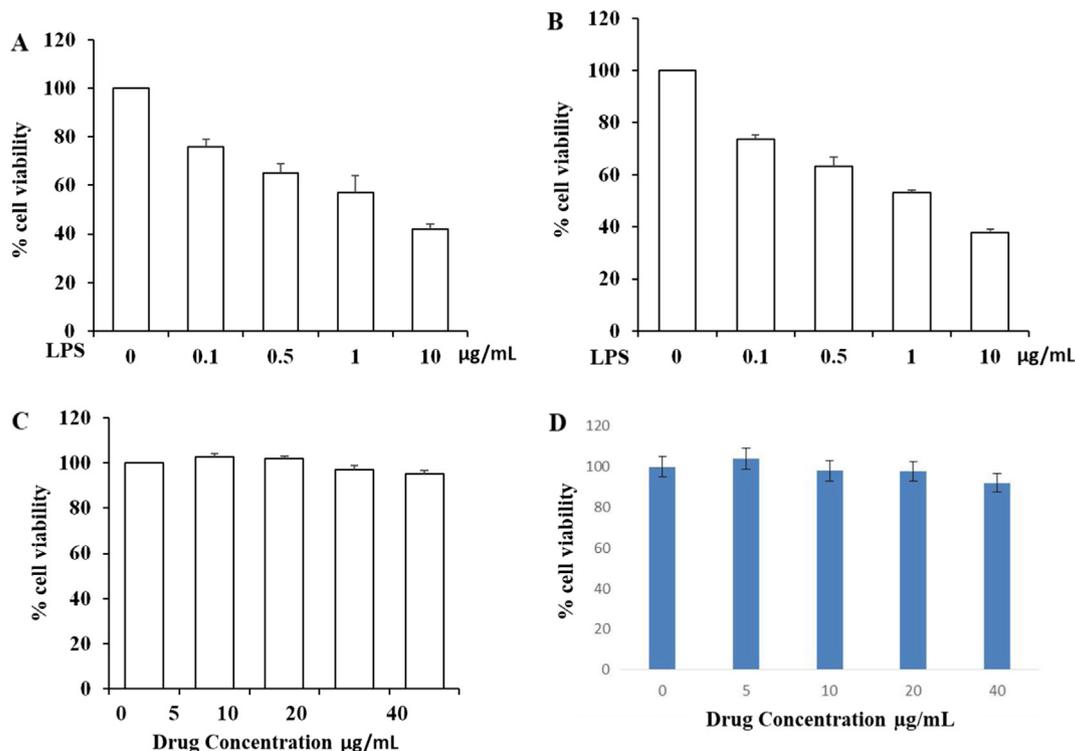
Fig. 5 Cytotoxic effect of synthesized Betulinic acid loaded PVA/Lig-g-MA nanoformulation on normal endothelial cells. Two type of normal endothelial cells Human Umbilical Vein Endothelial Cells (HUVEC) and Human Pulmonary Artery Endothelial Cells (HPAEC) were treated with different concentration of lipopolysaccharides (0–10 μg/ml) and Betulinic acid loaded PVA/Lig-g-MA nanoformulation ranging from 0 to 40 μg/ml and incubated for 24 h. The cells were then subjected to MTT assay and the results were statistically analyzed. Values are expressed as means ± S.D for six independent observation of each group. $p \leq 0.05$ considered to be statistically significant. A-HUVEC cells treated with/without LPS, B- HPAEC cells treated with/without LPS, C- HUVEC cells treated with/without betulinic acid nanoformulation, D- HPAEC cells treated with/without betulinic acid nanoformulation.

alcohol to methylacrylate grafted lignin. Further, natural compound of betulinic acid conjugated to the nanopolymer, which synthesized with polyvinyl alcohol/methylacrylate grafted lignin.

From FTIR studies of (a) Lig-g-MA, (b) PVA/Lig-g-MA and (c) Betulinic acid loaded PVA/Lig-g-MA electrospun nanofibers were characterized shown in Fig. 1(a)–(c). In this context, Fig. 1(a) attributed due to stretching vibration of —OH peaks of lignin, which fully distracted which indicated the lignin was successfully grafted on methyl acrylate monomer. Moreover, other characteristic peaks such as PVA/Lig-g-MA electrospun nanofibers given in 1737 cm^{-1}, 1366 cm^{-1} and 1207 cm^{-1} corresponded due to C=O, C—H and C—O groups of Lig-g-MA polymer. The FTIR spectrum of PVA/Lig-g-MA indicated that the PVA was successfully made hydrogen bond with Lig-g-MA polymer, which introduced new peak was appeared at —OH peak at 3229 cm^{-1} and the other peaks were appeared in same manner given in Fig. 1 (b). Further, the herbal drug of betulinic acid was successfully loaded on PVA/Lig-g-MA electrospun nanofibers through physical absorption of PVA/Lig-g-MA polymer. Thus, betulinic acid –OH stretching vibration of PVA/Lig-g-MA slightly shifted from 3229 cm^{-1} to 3314 cm^{-1}, which indicated Betulinic acid loaded PVA/Lig-g-MA electrospun nanofiber exposed in Fig. 1(c).

The morphological images of PVA/Lig-g-MA and Betulinic acid loaded PVA/Lig-g-MA nanofibers were evaluated using SEM and HR-TEM microscopy Fig. 2(A)–(D). The Fig. 2 (A) depicted that the fiber blended suspension of PVA/Lig-g-MA had some smooth and spider network like structure,

which average diameter of PVA/Lig-g-MA is ~1 μm. Afterwards, the herbal drug betulinic acid was loaded on PVA/Lig-g-MA through some hydrogen bonding interaction and physical interaction that showed some white spots of Fig. 1 (B). At last, the loaded BA was successfully covered with PVA/Lig-g-MA fiber. TEM analysis is another method to detect morphological structure of the compound, where this TEM morphological images of PVA/Lig-g-MA and Betulinic acid loaded PVA/Lig-g-MA correlated with SEM images shown in Fig. 2(C) and (D).

The XRD images of PVA/Lig-g-MA demonstrated in Fig. 3(a), where it showed no peaks due to by amorphous in nature. The crystalline pattern of electrospun nanofibers were detected by XRD studies. After, the herbal drug of betulinic acid was incorporated on electrospun nanofibers through physical interactions in Fig. 3(b). The BA-loaded PVA/Lig-g-MA exhibited some sharps peaks like 16.52 Å, 19.6 Å and 23.4 Å. This clearly indicated the betulinic acid peaks were successfully loaded on to electrospun nanofibers.

To detect the encapsulation efficiency of betulinic acid on PVA/Lig-g-MA electrospun nanofiber was used to UV–vis spectroscopy at the λ_{max} value of betulinic acid 205 nm illustrated in Fig. 4(a). In this work, the absorption intensity of betulinic acid was greatly diminished by increasing time. This due to the maximum amount of drug was easily encapsulated the electrospun nanofiber via hydrogen bonding of PVA/Lig-g-MA and betulinic acid. This UV–vis absorbance results suggested the entrapment efficiency was at 71.43% and the PVA/Lig-g-MA electrospun nanofiber portrayed in Fig. 4(a).
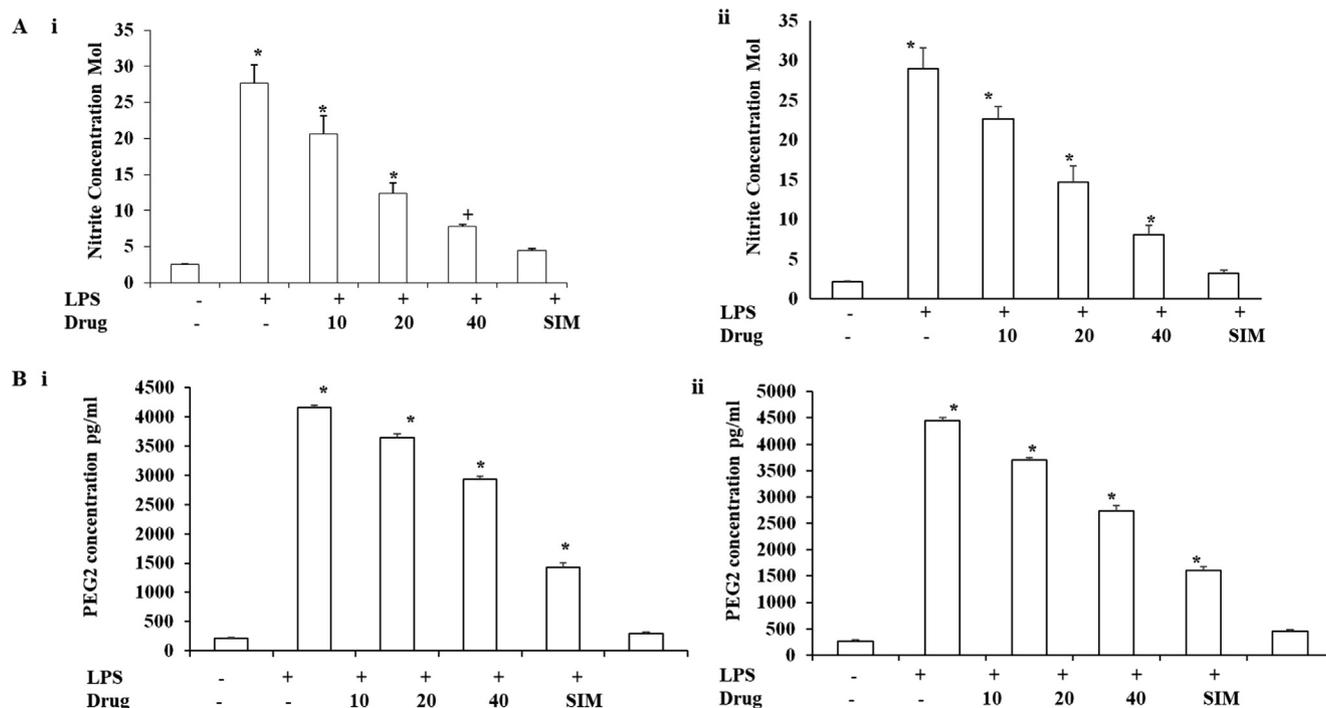
Fig. 6 Effect of synthesized Betulinic acid loaded PVA/Lig-g-MA nanoformulation against LPS induced inflammatory response. Human Umbilical Vein Endothelial Cells (HUVEC) and Human Pulmonary Artery Endothelial Cells (HPAEC) were treated with LPS and different concentration of Betulinic acid loaded PVA/Lig-g-MA nanoformulation ranging from 0 to 40 μg/ml and incubated for 24 h. The cells were then assessed for nitrite and PEG-2 concentration using commercially available kit. Values are expressed as means ± S.D for three independent observation of each group. P ≤ 0.05 considered to be statistically significant. A –Nitrate concentration of control and treated endothelial cells. B- PEG-2 Concentration of control and endothelial cells. i- HUVEC cell line, ii- HPAEC cell line.

In-vitro drug release of betulinic acid releasing profile has shown in Fig. 4 and the typical betulinic acid release rate of electrospun nanofiber was shown in Fig. 4(b) and (c). The drug release of betulinic acid loaded PVA/Lig-g-MA electrospun nanofiber was detected under different PBS solution such as 2.8 and 6.8 respectively and also by physiological local condition (pH-6.8) and intracellular acidic micro environment (pH-2.8) respectively. Under physiological condition (pH-6.8), the drug release rate of betulinic acid from PVA/Lig-g-MA electrospun nanofiber was very low and the cumulative amount of betulinic acid release was around (60%) for 24 h than acidic pH-2.8 that holds maximum drug release, noted on Fig. 4(d). It is speculated that the betulinic acid was controllably released on the electrospun nanofiber under the acidic condition in tumor site.

Antiatherosclerotic activity of the formulated nanodrug was assessed in both *in vitro* and *in vivo* conditions. Cytokines plays a vital function in the induction of atherosclerosis start from the disruption of endothelial cells function to till plaques disruption. Hence, most of the commercially available anti atherosclerotic drugs targets the inflammatory cytokines to treat atherosclerosis (Singh et al., 2009).

Fig. 5 signified the results of cytotoxic effect induced by lipopolysaccharides (LPS) and Betulinic acid loaded PVA/Lig-g-MA nanoformulation on two different type of normal endothelial cells HUVEC and HPAEC. Dose dependent diminution in cell viability was observed in the LPS treated cells. Both HUVEC and HPAEC cells treated with 10 µg/ml of LPS showed 50% of cell death whereas nanoformulation treated showed none of the noticeable variations in their cell viability compared to the untreated cells.

The inhibitory effect of Betulinic acid loaded PVA/Lig-g-MA nanoformulation against the nitrite production induced by LPS were represented in the Fig. 6(A). Simultaneous treatment of nanoformulation along with LPS significantly reduced nitrite production induced by LPS. Both HUVEC and HPAEC cells treated with 40 µg/ml Betulinic acid loaded PVA/Lig-g-MA nanoformulation showed significant reduction in nitrite production rather than reduction induced by standard drug cholesterol reducing drug, simvastatin.

Prostaglandins perform crucial function in developing atherosclerosis by mediating inflammation in vascular tissue and increased the levels of PGE2. In our current exploration, the Betulinic acid loaded PVA/Lig-g-MA nanoformulation effectively inhibited the production of PGE2 by LPS treatment in a dose dependent manner (Fig. 6(B)).

As cytokines secrete due to inflammation stimuli by endothelial cells, the inhibitory effect of Betulinic acid loaded PVA/Lig-g-MA nanoformulation decreased the secretion of proinflammatory cytokines TNFα (Fig. 7(A)), IL-6 (Fig. 7(B)) and IL-1β (Fig. 7(C)) in both HUVEC and HPAEC cells compared to untreated cells. In dose dependent nanoformula-
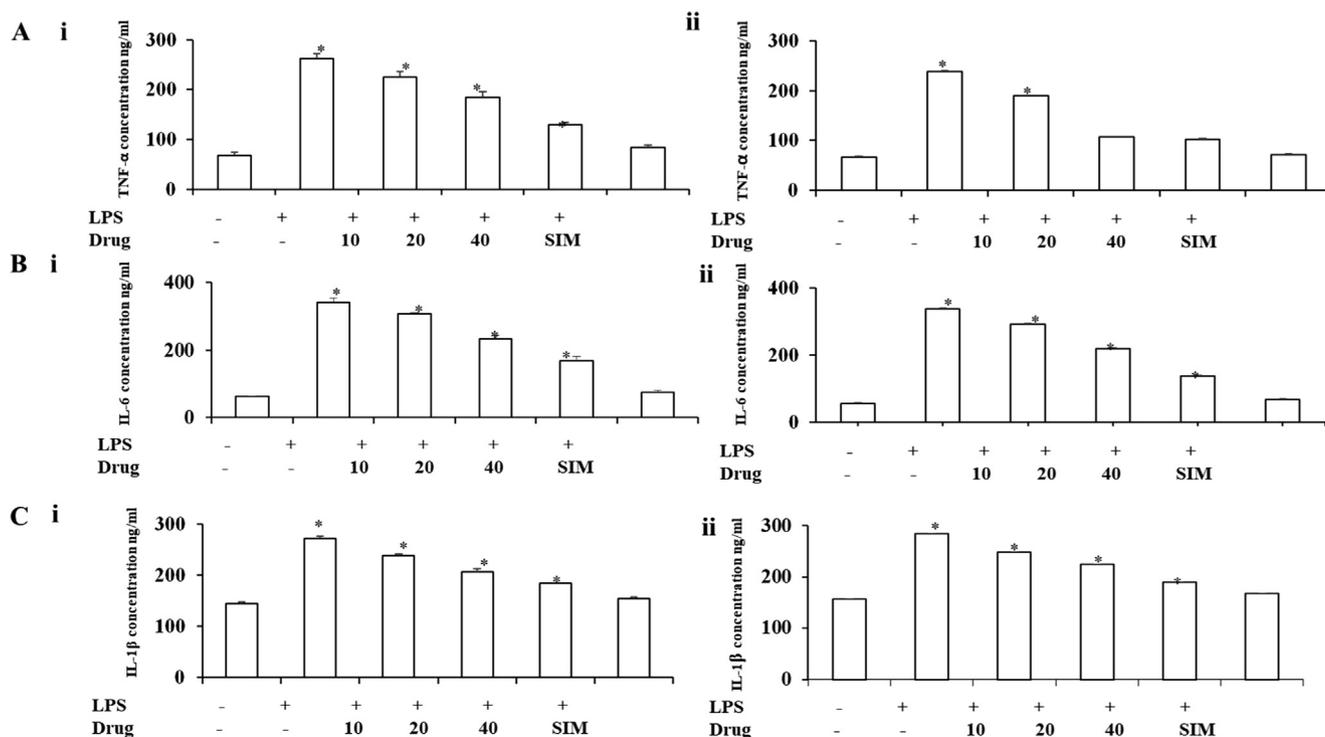
Fig. 7 Effect of synthesized Betulinic acid loaded PVA/Lig-g-MA nanoformulation against LPS induced inflammatory cytokines. Human Umbilical Vein Endothelial Cells (HUVEC) and Human Pulmonary Artery Endothelial Cells (HPAEC) were treated with LPS and different concentration of Betulinic acid loaded PVA/Lig-g-MA nanoformulation ranging from 0 to 40 µg/ml and incubated for 24 h. The cells were then assessed for TNFα, IL-6 and IL-1β using commercially available kit. Values are expressed as means ± S.D for three independent observation of each group. p ≤ 0.05 considered to be statistically significant. A – TNF-α concentration of control and treated endothelial cells, B – IL-6 concentration of control and treated endothelial cells, C – IL-1β concentration of control and treated endothelial cells. i- HUVEC cell line, ii- HPAEC cell line.

tion treatment, there was similar type of inhibitory effect was observed in both HUVEC and HPAEC cells. Particularly, 40 μg/ml nanoformulation treated cells showed decreased levels of proinflammatory cytokines as that of standard drug simvastatin treated cells.

In the cytotoxic study, our nanoformulation expressed no cytotoxicity on both normal endothelial cells HUVEC and HPAEC, On the other hand, it reduced the level of nitrate and PEG2 induced by lipopolysaccharides. Vascular smooth muscle cells secretes cytokines tumor necrosis factor-α (TNF-α), interleukin (IL)-1 and IL-6, which are pro atherogenic in nature (Csuk, 2014). Remarkably in both endothelial, the betulinic acid loaded PVA/Lig-g-MA nanoformulation effectively inhibited the secretion of proatherogenic cytokines induced by LPS, which witnessed the nanoformulation inhibits atherogenic activity.

NF-κB signaling always acts as a master switch in inflammatory process which channelizes various other inflammatory signaling molecules (Zhang et al., 2015). They regulates the proatherogenic cytokines and inhibits the formation of atherosclerotic plaque, matrix deposition, leukocyte-endothelial adhesion there by prevent the coronary arteries to form atherosclerosis (Ali-Seyed et al., 2016). The p38 mitogen-activated protein kinase (p38MAPK) is triggered by the pro atherogenic cytokines like TNFα and interleukins (Csuk, 2014). IκB are the signaling molecule that inhibits the NF-κB protein and retains them as inactive NF-κB in the cytoplasm (Thakur and Thakur, 2015). But, stimuli like inflamma-

tory cytokines, which in turn phosphorylates IκκB to phosphorylates IκB signaling protein and thereby releasing active NF-κB into the nucleus (Sánchez et al., 2016). In immunoblotting analysis, the HUVEC cells cytoplasmic fraction clearly depicted the LPS induced the phosphorylation of inhibitory kinases, IκκB-α and its downstream molecule IκB-α there by activating NF- κ β towards the nucleus (Fig. 8A). On the contrary, the nanoformulation treated cells showed decreased in the phosphorylation of inhibitory kinases and increased levels of inactive NF- κ β in cytoplasmic fraction. It is confirmed that there was steady decrease in NF- κ β and the transcription factor c jun protein and in nucleus fraction of treated cells (Fig. 8(B)) which confirms that Betulinic acid loaded PVA/Lig-g-MA effectively inhibited the proatherogenic cytokines thereby inhibited the stimulation of NF-κB/p65 protein.

In another way, the activation of JNK signaling molecules induce NF-κB signaling proteins and phosphorylation of IκB kinase proteins, which leads nuclear translocation of NF-κB and eventually induce atherosclerosis (Vogl and Tirrell, 1979; Gaaz et al., 2015). MEKK1, MEKK2, ERK1/2, TGF- β –activating kinase 1 (TAK1) and NF-κB stimulated kinase phosphorylates IκB kinase thereby activating NF-κB (Ridker and Lüscher, 2014; Tedgui and Mallat, 2006). Fig. 9 represented the levels of MAP/JNK signaling proteins in LPS induced and nanoformulation treated HUVEC cells. There was a significant decrease in the status of ERK1/2, AKT, JNK, p38 phosphorylation observed in nanoformulation treated cells
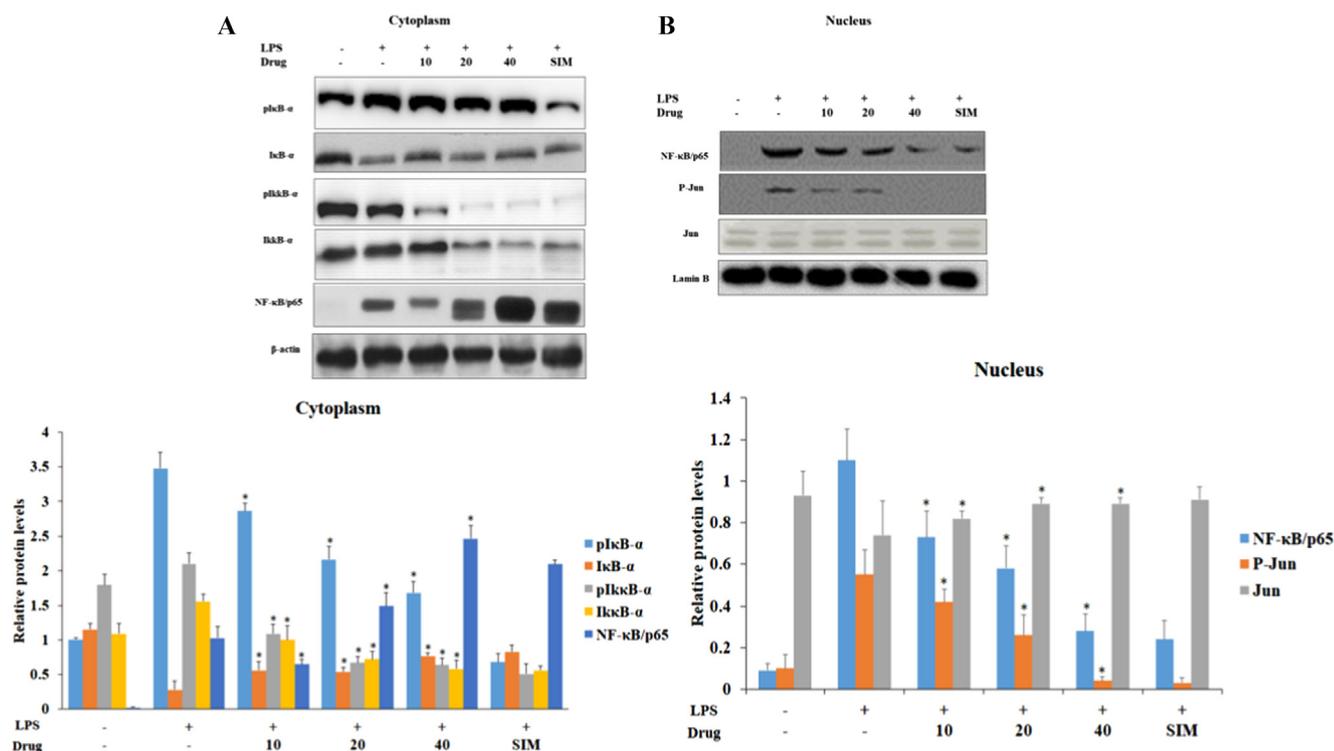
Fig. 8 Effect of synthesized Betulinic acid loaded PVA/Lig-g-MA nanoformulation on LPS induced NF- κ β signaling in HUVEC endothelial cell line. The control and treated cells were subjected to cytoplasmic and nuclear fractionation. 40 μg of total protein from control and treated group cytoplasmic fraction were subjected to electrophoresis and immunoblotting analysis with specific NF-κB signaling proteins pIκB-α, IκB-α, pIκκB-α, IκκB-α, NF-κB/p65. 40 μg of total protein from control and treated group nuclear fraction were subjected to electrophoresis and immunoblotting analysis with NF-κB/p65, Jun and pJun proteins. Values are expressed as means ± S.D for three independent observation of each group. '*' p ≤ 0.05 considered to be statistically significant.

than LPS alone induced cells. Specifically in 40 µg/ml nanoformulation treated, the levels of phosphorylated AKT, JNK, and p38 were drastically decreased as same as standard drug simvastatin treated cells.

Since the hypercholesterolemia is the main triggering agent of atherosclerotic plaque formation, we used rat model by feeding them high fat diet for a period of 30 days. This was used to detect the potency of Betulinic acid loaded PVA/Lig-g-MA by also treat the same rat model with nanoformulation. High fat diet increases the statuses of total cholesterol, triglycerides, low and very low density cholesterol and decreases the high density cholesterol (Brand et al., 1997), which are the key factor for the development of atherosclerosis. In particular, LDL and VLDL acts as a inducer of atherosclerotic plaque formation that leads to lipid peroxidation in coronary arteries (Tang and Raines, 2005; Ghosh and Baltimore, 1990). Fig. 10, evidenced the levels of total cholesterol, total glyceride, HDL cholesterol, LDL cholesterol and VLDL cholesterol in control and nanoformulation treated rats. In this, these values were

decreased in both low and high dose Betulinic acid loaded PVA/Lig-g-MA nanoformulation treated rat when compared to atherosclerosis induced rats.

This increased levels of low density lipoproteins consecutively trigger macrophages to accrete interleukin, which are atherogenic in nature. Interleukin 1β stimulates the production of platelet derived growth factor to initiate the proliferation of vascular endothelial and smooth muscle cells that leading to form artherogenesis (Abbate et al., 2020). Both IL-18 and IL-8 are the potent agent for the initiation of atherosclerotic plaque but especially, IL-8 effectively attracts neutrophils that induce endothelial monocyte adhesion and vascular smooth muscle migration, leading to the formation of atherosclerotic plaque (Verma et al., 1995; Yang et al., 2001; Nakano et al., 1998; Ninomiya-Tsuji et al., 1999; Shrivastavaa et al., 2013). Hence, inhibiting these atherogenic molecules may be an effective treatment for atherosclerosis. Remarkably, our present study on synthesized nanoformulation, it potentially inhibited the secretion of interleukins because of high fat diet thereby
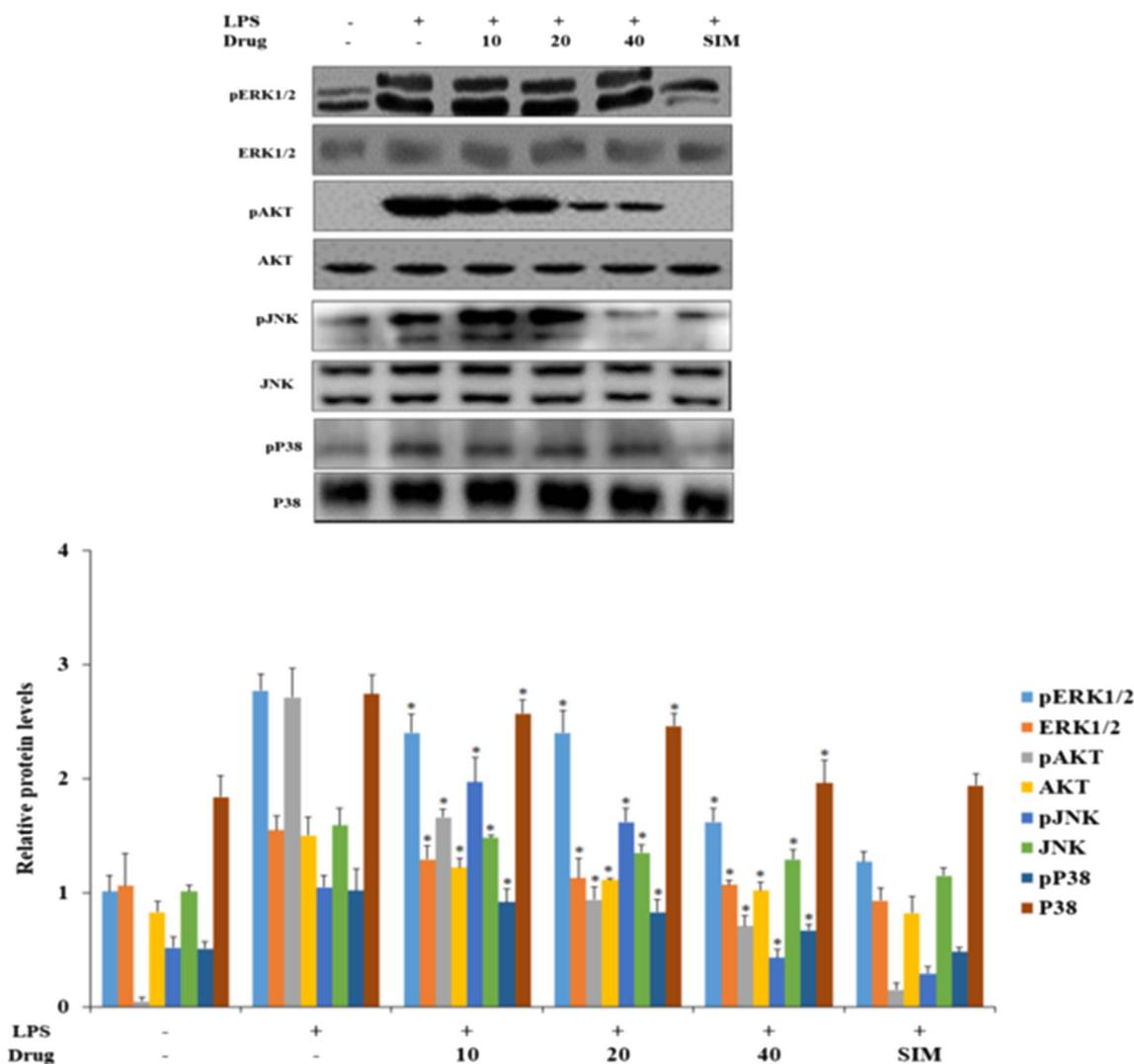
Fig. 9 Effect of synthesized Betulinic acid loaded PVA/Lig-g-MA nanoformulation on LPS induced MAP/JNK signaling in HUVEC endothelial cell line. 40 µg of total protein from control and treated group cells were subjected to electrophoresis and immublotting analysis with specific MAP/JNK signaling proteins ERK1/2, pERK1/2, pAKT, AKT, pJNK, JNK, p38, Pp38. Values are expressed as means ± S.D for three independent observation of each group. '*' $p \leq 0.05$ considered to be statistically significant.
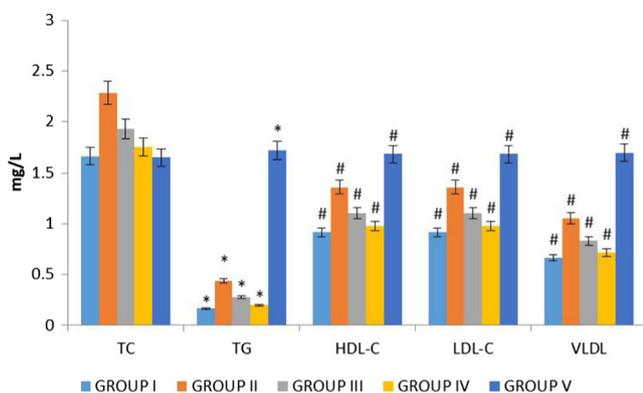
Fig. 10 Effect of synthesized Betulinic acid loaded PVA/Lig-g-MA nanoformulation on lipid profile in high fat diet induced atherosclerotic rat model. The blood samples were collected and subjected to analysis of total cholesterol, total glyceride, HDL cholesterol, LDL cholesterol and VLDL cholesterol using commercially available kits. Values are expressed as means ± S.D for six independent observation of each group. '*' p ≤ 0.05 considered as significant when compared to the control and '#' p ≤ 0.05 considered as significant when compared to the atherosclerosis group.

preventing the rats from atherosclerosis induction. The reduction in inflammation is directly correlate with the levels of C-reactive proteins, where the statin effectively reduces the inflammation by decreasing the level LDL (Lusis, 2000). The decreased level of C-reactive protein in the nanoformulation treated high fat diet rats confirmed the anti-atherosclerotic property. Altogether, our nanoformulation effectively inhibited the induction interleukins (Fig. 11(A)) and appreciably reduced the levels of C reactive protein in nanoformulation treated group compared to the high fat diet alone group.

Numerous studies have reported that patients with non-alcoholic fatty liver ailment has limited vasodilation and more prone to atherosclerosis than the normal people (Mohammed, 2002; Libby, 2017). This alteration of liver functioning enzymes leads to thickening of carotid artery that cause atherosclerotic plaques. (Elhage et al., 2003) Fig. 11(B) exem-
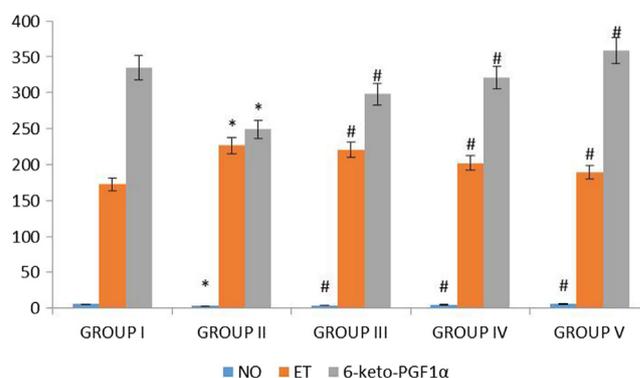
Fig. 12 Effect of synthesized Betulinic acid loaded PVA/Lig-g-MA nanoformulation on vasodilators in high fat diet induced atherosclerotic rat model. The blood samples were collected and subjected to analysis of nitric oxide, endothelin and 6 keto PGF 1α using commercially available kits. Values are expressed as means ± S.D for six independent observation of each group. '*' p ≤ 0.05 considered as significant when compared to the control and '#' p ≤ 0.05 considered as significant when compared to the atherosclerosis group.

plified significant fall in the levels of ALT, ALP, AST and LDH in the nanoformulation treated rats as compared to high fat diet alone rats. But interestingly, the levels of liver function enzymes in high dose nanoformulation treated rats was similar to the simvastatin, standard drug administered rats. On the whole, it clearly depicted the nanoformulation decreases the lipid levels thereby prevented the liver inflammation triggered by high fat diet.

Vasodilators such as nitric oxide, endothelin perform master function in inhibiting the induction of atherosclerosis in hypercholesterolemia and hypertension patients (Mallat et al., 2001). Another report stated that the inhibition of L-arginine NO signaling the induction of atherosclerotic lesions in hypercholestremic rabbits and also in the LDL receptor deficient mice (Gerszten et al., 1999; Liu et al., 1997). The vasoactive agents NO and endothelin effectively regulated the vascular structure, which deregulated by the increased lipids
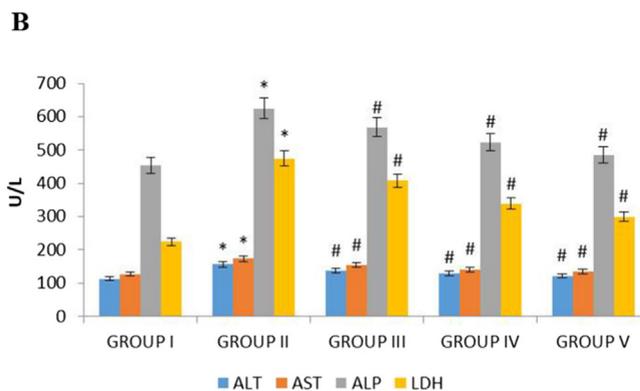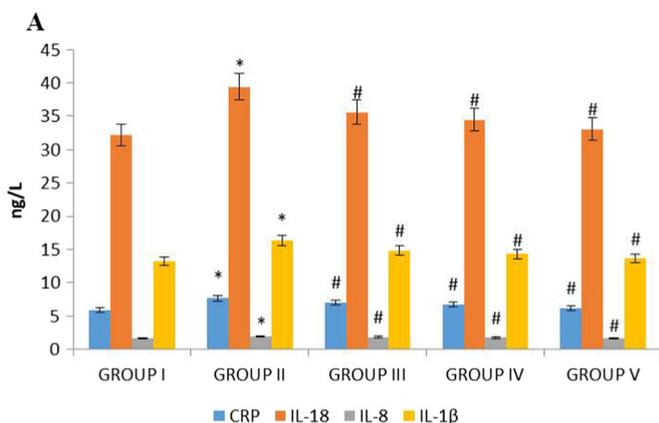
Fig. 11 Effect of synthesized Betulinic acid loaded PVA/Lig-g-MA nanoformulation on inflammatory interleukin and liver function enzymes in high fat diet induced atherosclerotic rat model. The blood samples were collected and subjected to analysis of (A) C-reactive protein, IL-1β, IL-8 and IL-18 (B) ALT, AST, ALP and LDH levels using commercially available kits. Values are expressed as means ± S. D for six independent observation of each group. '*' p ≤ 0.05 considered as significant when compared to the control and '#' p ≤ 0.05 considered as significant when compared to the atherosclerosis group.
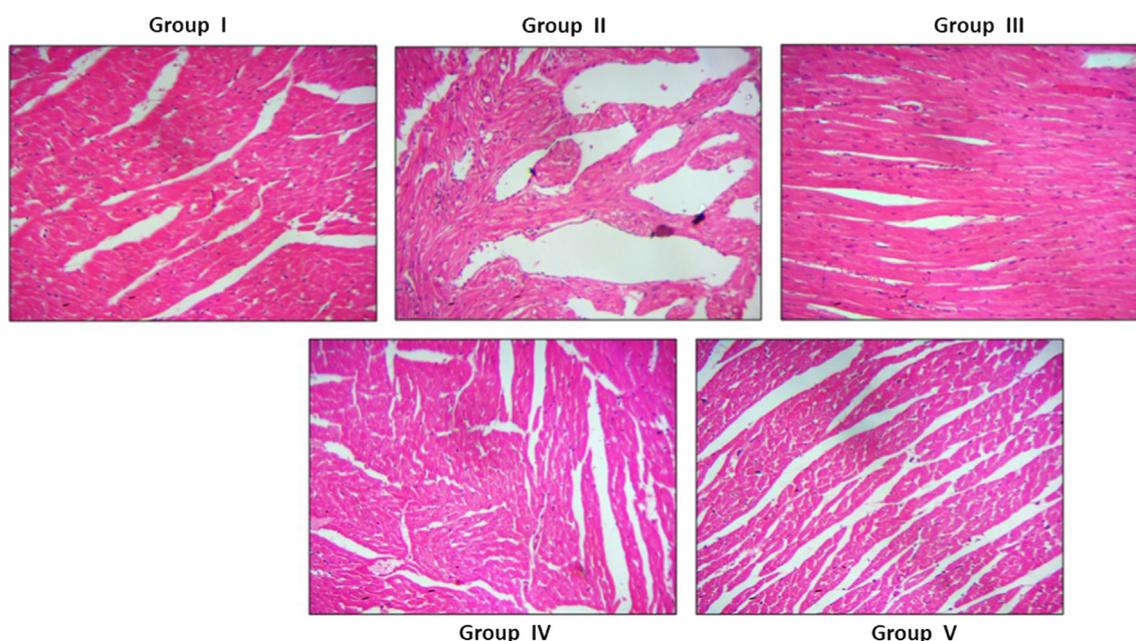
Fig. 13 Effect of synthesized Betulinic acid loaded PVA/Lig-g-MA nanoformulation on cardiac tissue histomorphometry in high fat diet induced atherosclerotic rat model. The cardiac muscle of control and experimental rats were processed for histological analysis and sectioned into slices of 5 μm thickness. The sectioned slides were stained with haematoxylin and eosin stains. The stained slides were viewed under light microscope and photographed. The experiments were performed in triplicates.

levels (Yue et al., 1993). In our study, the low and high dose nanoformulation treated rats shown appreciably enhanced level of vasodilators nitric oxide, endothelin and 6 keto PGF-1α than compared to the high fat diet supplemented rats (Fig. 12). But, it was significantly equal to the standard drug simvastatin treated rats (Yue et al., 1993). Succeeding, nanoformulation treatment confront the increase of another vasoactive mediator 6-keto-Prostaglandin F1α, which is a metabolite of prostacyclin that inhibits the platelet aggregation in vascular tissues. Therefore, our nanoformulation treatment significantly increased the levels of all three vasodilators and thereby preventing the vascular tissue from the induction atherosclerotic lesions.

The H&E stained cardiac tissue photomicrographs of control and nanoformulation treated rats were illustrated in Fig. 13. The regular pattern of cardiac myofibres with oval shaped nuclei located centrally on the cardiomyocytes were seen in control (group I), standard drug simvastatin treated (group V), simultaneous low (group III) and high dose (group IV) nanoformulation treated rat cardiac tissue. Whereas irregular pattern of cardiac myofibres were observed in cardiac tissue of atherosclerosis induced rats (group II). The histopathological evidence of coronary arteries clearly states that the Betulinic acid loaded PVA/Lig-g-MA nanoformulation prevented degeneration of myocardial cells caused by deregulated lipid levels induced by high fat diet.

4. Conclusion

In conclusion, the physical characteristic analysis, *in vitro* drug releasing capacity of Betulinic acid loaded PVA/Lig-g-MA nanoformulation suggested that it would be an ideal drug for medication. The cytotoxicity analysis of Betulinic acid loaded

PVA/Lig-g-MA nanoformulation on normal endothelial cells proven its nontoxic and it also effectively inhibited the levels of inflammatory cytokines via inhibiting the NFκB and JNK signaling pathway. By following, the *in vivo* analysis also supported. The data from *in vitro* studies, showed it effectively subdued the levels of lipids, interleukins and increased the levels of vasodilators thereby preventing the myocardial cells from degeneration. It also witnessed hepatoprotective effect against high fat diet induced liver damage. Over all our results authentically proved that the Betulinic acid loaded PVA/Lig-g-MA nanoformulation would be a cost effective, biodegradable, non-toxic and potential anti atherosclerotic nanodrug.

Declaration of Competing Interest

The authors declare that they have no known competing financial interests or personal relationships that could have appeared to influence the work reported in this paper.

Acknowledgement

References

Abbate, A., Toldo, S., Marchetti, C., Kron, J., Tassel, B.W.V., Dinarello, C.A., 2020. Interleukin-1 and the inflammasome as therapeutic targets in cardiovascular disease. Circ. Res. 126 (9), 1260–1280.

Ali-Seyed, M., Jantan, I., Vijayaraghavan, K., Bukhari, S.N., 2016. Betulinic Acid: recent advances in chemical modifications, effective

delivery, and molecular mechanisms of a promising antiherbal therapy. Chem. Biol. Drug Des. 87 (4), 517–536.

Benjamin, E.J., Muntner, P., Alonso, A., Bittencourt, M.S., Callaway, C.W., Carson, A.P., Chamberlain, A.M., Chang, A.R., Cheng, S., Das, S.R., Delling, F.N., Djousse, L., Elkind, M.S.V., Ferguson, J. F., Fornage, M., Jordan, L.C., Khan, S.S., Kissela, B.M., Knutson, K.L., Kwan, T.W., Lackland, D.T., Lewis, T.T., Licht-man, J.H., Longenecker, C.T., Loop, M.S., Lutsey, P.L., Martin, S. S., Matsushita, K., Moran, A.E., Mussolino, M.E., Oflaherty, M., Pandey, A., Perak, A.M., Rosamond, W.D., Roth, G.A., Sampson, U.K.A., Satou, G.M., Schroeder, E.B., Shah, S.H., Spartano, N.L., Stokes. A., Tirschwell, D.L., Tsao, C.W., Turakhia, M.P., Van Wagner, L.B., Wilkins, J.T., Wong, S.S., Virani, S.S., 2019. American Heart Association Council on Epidemiology and Prevention Statistics Committee and Stroke Statistics Subcommit-tee. Heart Disease and StrokeStatistics-2019 Update: A Report From the American Heart Association. Circulation 139(10), e56–e528.

Brand, K., Page, S., Walli, A.K., Neumeier, D., Baeuerle, P.A., 1997. Role of nuclear factor-κB in atherogenesis. Exp. Phy. 82 (2), 297–304.

Csuk, R., 2014. Betulinic acid and its derivatives: a patent review (2008–2013). Expert Opin Ther Pat. 24 (8), 913–923.

de Melo, C.L., Queiroz, M.G., Arruda Filho, A.C., Rodrigues, A.M., de Sousa, D.F., Almeida, J.G., Pessoa, O.D., Silveira, E.R., Menezes, D.B., Melo, T.S., Santos, F.A., Rao, V.S., 2009. Betulinic acid, a natural pentacyclic triterpenoid, prevents abdominal fat accumulation in mice fed a high-fat diet. J. Agric. Food Chem. 57 (19), 8776–8781.

Elhage, R., Jawien, J., Rudling, M., Ljunggren, H.G., Takeda, K., Akira, S., Bayard, F., Hansson, G.K., 2003. Reduced atheroscle-rosis in interleukin-18 deficient apolipoprotein E-knockout mice. Cardiovasc. Res. 59 (1), 234–240.

Faralli, Adele, Shekarforoush, Elhamalsadat, Ajalloueian, Fatemeh, Mendes, Ana C., Chronakis, Ioannis S., 2019. In vitro permeability enhancement of curcumin across Caco-2 cells monolayers using electrospun xanthan-chitosan nanofibers. Carbohydrate Polym. 206, 38–47.

Figueiredo, P., Lintinen, K., Hirvonen, J.T., Kostiainen, M.A., Santos, H.A., 2018. Properties and chemical modifications of lignin: towards lignin-based nanomaterials for biomedical applica-tions. Prog. Mater. Sci. 93, 233–269.

Gaaz, T.S., Sulong, A.B., Akhtar, M.N., Kadhum, A.A., Mohamad, A.B., Al-Amiery, A.A., 2015. Properties and applications of polyvinyl alcohol, halloysite nanotubes and their nanocomposites. Molecules 20 (12), 22833–22847.

Gerszten, R.E., Garcia-Zepeda, E.A., Lim, Y.C., Yoshida, M., Ding, H.A., Gimbrone Jr, M.A., Luster, A.D., Luscinskas, F.W., Rosenzweig, A., 1999. MCP-1 and IL-8 trigger firm adhesion of monocytes to vascular endothelium under flow conditions. Nature 398 (6729), 718–723.

Ghosh, S., Baltimore, D., 1990. Activation in vitro of NF-κB by phosphorylation of its inhibitor IκB. Nature 344 (6267), 678–682.

Godugu, C., Patel, A.R., Doddapaneni, R., Somagoni, J., Singh, M., 2014. Approaches to improve the oral bioavailability and effects of novel anticancer drugs berberine and betulinic acid. PLoS ONE 9, (3) e89919.

Gu, Xiaohua, Cao, Rui, Li, Yan, Liu, Siwen, Wang, Zhigang, Feng, Shuqin, Li, Fu, Lyu, Shiwei, 2019. Three-component antibacterial membrane of poly(butylene carbonate), poly(lactic acid) and chitosan prepared by electrospinning. Mater. Technol. 34, 463–470.

Guo, G., Li, S., Wang, L., Ren, S., Fang, G., 2013. Separation and characterization of lignin from bio-ethanol production residue. Bioresour. Technol. 135, 738–741.

Harwansh, R.K., Mukherjee, P.K., Biswas, S., 2017. Nanoemulsion as a novel carrier system for improvement of betulinic acid oral bioavailability and hepatoprotective activity. J. Mol. Liquids 237, 361–371.

Heidari, M., Bahrami, S.H., Ranjbar-Mohammadi, M., et al, 2019. Smart electrospun nanofibers containing PCL/gelatin/graphene oxide for application in nerve tissue engineering. Mater. Sci. Eng. C. 103, 109768.

Hobzova, Radka, Hampejsova, Zuzana, Cerna, Tereza, Hrabeta, Jan, Venclikova, Kristyna, Jedelska, Jarmila, Bakowsky, Udo, Bosa-kova, Zuzana, Lhotka, Miloslav, Vaculin, Simon, Franek, Milo-slav, Steinhart, Milos, Kovarova, Jana, Michalek, Jiri, Sirc, Jakub, 2019. Poly(d, l-lactide)/polyethylene glycol micro/nanofiber mats as paclitaxel-eluting carriers: preparation and characterization of fibers, in vitro drug release, antiangiogenic activity and tumor recurrence prevention. Mater. Sci. Eng., C 8, 982–993.

Huang, C., Tang, S., Zhang, W., Tao, Y., Lai, C., Li, X., Yong, Q., 2018. Unveiling the structural properties of lignin–carbohydrate complexes in bamboo residues and its functionality as antioxi-dants and immunostimulants. ACS Sustain. Chem. Eng. 6, 12522–12531.

Huang, C., Wang, X., Liang, C., Jiang, X., Yang, G., Xu, J., Yong, Q., 2019. A sustainable process for procuring biologically active fractions of high-purity xylooligosaccharides and water-soluble lignin from Moso bamboo prehydrolyzate. Biotechnol. Biofuels 12, 189.

Hussein-Al-Ali, Samer Hasan, Arulselvan, Palanisamy, Fakurazi, Sharida, Hussein, Mohd Zobir, 2014. The in vitro therapeutic activity of betulinic acid nanocomposite on breast cancer cells (MCF-7) and normal fibroblast cell (3T3). J. Mater. Sci. 49, 8171–8182.

Jatoi, Abdul Wahab, Ogasawara, Hiroshi, Kim, Ick Soo, Ni, Qing-Qing, 2019. Polyvinyl alcohol nanofiber based three phase wound dressings for sustained wound healing applications. Mater. Lett. 241, 168–171.

Jeyaraj, Murugaraj, Praphakar, Rajendran Amarnath, Rajendran, Chinnusamy, Ponnamma, Deepalekshmi, Sadasivuni, Kishor Kumar, Munusamy, Murugan A., Rajan, Mariappan, 2016. Surface functionalization of natural lignin isolated from Aloe barbadensis Miller biomass by atom transfer radical polymeriza-tion for enhanced anticancer efficacy. RSC Adv. 6, 51310.

José, L., 2008. Arias, novel strategies to improve the anticancer action of 5-fluorouracil by using drug delivery systems. Molecules 13, 2341.

Kadavil, Hana, Zagho, Moustafa, Elzatahry, Ahmed, Altahtamouni, Talal, 2019. Sputtering of electrospun polymer-based nanofibers for biomedical applications: a perspective. Nanomaterials 9, 77.

Kalani, M.M., Nourmohammadi, J., Negahdari, B., et al, 2019. Electrospun core-sheath poly(vinyl alcohol)/silk fibroin nanofibers with Rosuvastatin release functionality for enhancing osteogenesis of human adipose-derived stem cells. Mater. Sci. Eng.: C 99, 129–139.

Libby, P., 2017. Interleukin-1 beta as a target for atherosclerosis therapy: the biological basis of CANTOS and beyond. J. Am. Coll. Cardiol. 70 (18), 2278–2289.

Liu, Y., Hultén, L.M., Wiklund, O., 1997. Macrophages isolated from human atherosclerotic plaques produce IL-8, and oxysterols may have a regulatory function for IL-8 production. Arterioscler. Thromb. Vasc. Biol. 17 (2), 317–323.

Lusis, A.J., 2000. Atherosclerosis. Nature 407 (6801), 233–241.

Ma, K., Rozet, Y., Tamada, J., Yao, Q., Ni, Q., 2019. Multi-layer nanofibrous tubes with dual drug-release profiles for vascular graft engineering. J. Drug Delivery Sci. Technol.

Mallat, Z., Corbaz, A., Scoazec, A., Graber, P., Alouani, S., Esposito, B., Humbert, Y., Chvatchko, Y., Tedgui, A., 2001. Interleukin-18/interleukin-18 binding protein signaling modulates atherosclerotic lesion development and stability. Circ. Res. 89 (7), E41–E45.

Martín-Sampedro, R., Santos, J.I., Fillat, U., Wicklein, B., Eugenio, M.E., Ibarra, D., 2019. Characterization of lignins from Populus alba L. generated as by-products in different transformation processes: Kraft pulping, organosolv and acid hydrolysis. Int. J. Biol. Macromol. 126, 18–29.

Mathew, L.E., Rajagopal, V., Helen, A., 2017. Betulinic acid and fluvastatin exhibits synergistic effect on toll-like receptor-4 mediated antiatherogenic mechanism in type II collagen induced arthritis. Biomed. Pharmacother. 93, 681–694.

McLaren, J.E., Michael, D.R., Ashlin, T.G., Ramji, D.P., 2011. Cytokines, macrophage lipid metabolism and foam cells: Implications for cardiovascular disease therapy. Prog. Lipid Res. 50, 331–347.

Mohammed, M.H., 2002. Mini review experimental atherosclerosis: a historical overview. Life Sci. 70, 855–865.

Nakano, H., Shindo, M., Sakon, S., Nishinaka, S., Mihara, M., Yagita, H., Okumura, K., 1998. Differential regulation of IkappaB kinase alpha and beta by two upstream kinases, NF-kappaB-inducing kinase and mitogen-activated protein kinase/ERK kinase kinase-1. Proc. Natl. Acad. Sci. USA 95 (7), 3537–3542.

Nayani, Karthik, Katepalli, Hari, Sharma, Chandra S., Sharma, Ashutosh, Patil, Sandip, Venkataraghavan, R., 2012. Electrospinning combined with nonsolvent-induced phase separation to fabricate highly porous and hollow submicrometer polymer fibers. Ind. Eng. Chem. Res. 51, 1761–1766.

Ninomiya-Tsuji, J., Kishimoto, K., Hiyama, A., Inoue, J., Cao, Z., Matsumoto, K., 1999. The kinase TAK1 can activate the NIK-I kappaB as well as the MAP kinase cascade in the IL-1 signalling pathway. Nature 398 (6724), 252–256.

Pahan, K., 2006. Lipid-lowering drugs. Cell Mol Life Sci. 63 (10), 1165–1178.

Ridker, P.M., Lüscher, T.F., 2014. Anti-inflammatory therapies for cardiovascular disease. Eur. Heart J. 35 (27), 1782–1791.

Sadri, M., Arab-Sorkhi, S., Vatani, H., Bagheri-Pebdeni, A., 2015. New wound dressing polymeric nanofiber containing green tea extract prepared by electrospinning method. Fibers Polym. 16, 1742–1750.

Safaee-Ardakani, Mohammad Reza, Zarmi, Ashrafalsadat Hatamian, Sadat, Seyedeh Mahdieh, Mokhtari-Hosseini, Zahra Beagom, Hosseinzadeh, Bahman Ebrahimi, Rashidiani, Jamal, Kooshki, Hamid, 2019. Electrospun Schizophyllan/polyvinyl alcohol blend nanofibrous scaffold as potential wound healing. Int. J. Biol. Macromol. 127, 27–38.

Sánchez, R., Espinosa, E., Domínguez-Robles, J., Loaiza, J.M., Rodríguez, A., 2016. Isolation and characterization of lignocellulose nanofibers from different wheat straw pulps. Int. J. Biol. Macromol. 92, 1025–1033.

Santos, J.I., Fillat, U., Martín-Sampedro, R., Eugenio, M.E., Negro, M.J., Ballesteros, I., Rodríguez, A., Ibarra, D., 2017. Evaluation of lignins from side-streams generated in an olive tree pruning-based biorefinery: bioethanol production and alkaline pulping. Int. J. Biol. Macromol. 105, 238–251.

Santos, S.C., Miguel, C., Domingues, I., Calado, A., Zhu, Z., Wu, Y., Dias, S., 2007. VEGF and VEGFR-2 (KDR) internalization is required for endothelial recovery during wound healing. Exp Cell Res. 313 (8), 1561–1574.

Shrivastava, A., Chaturvedi, U., Singh, S.V., 2013. Lipid lowering and antioxidant effect of miglitol in triton treated hyperlipidemic and high fat diet induced obese rats. Lipids 48, 597–607.

Singh, V., Tiwari, R.L., Dikshit, M., et al, 2009. Models to study atherosclerosis: A mechanistic insight. Curr. Vasc. Pharmacol. 7 (1), 75–109.

Subramani, C., Rajakkannu, A., Rathinam, A., Gaidhani, S., Raju, I., Kartar Singh, D.V., 2017. Anti-atherosclerotic activity of root bark of Premna integrifolia Linn. in high fat diet induced atherosclerosis model rats. J Pharm Anal. 7 (2), 123–128.

Takada, Y., Aggarwal, B.B., 2003. Betulinic acid suppresses carcinogen-induced NF-kappa B activation through inhibition of I kappa B alpha kinase and p65 phosphorylation: abrogation of cyclooxygenase-2 and matrix metalloprotease-9. J. Immunol. 171 (6), 3278–3286.

Tang, J., Raines, E.W., 2005. Are suppressors of cytokine signaling proteins recently identified in atherosclerosis possible therapeutic targets?. Trends Cardiovasc. Med. 15 (7), 243–249.

Tedgui, A., Mallat, Z., 2006. Cytokines in atherosclerosis: pathogenic and regulatory pathways. Physiol. Rev. 86 (2), 515–581.

Thakur, V.K., Thakur, M.K., 2015. Recent advances in green hydrogels from lignin: a review. Int. J. Biol. Macromol. 72, 834–847.

Verma, I.M., Stevenson, J.K., Schwarz, E.M., Van Antwerp, D., Miyamoto, S., 1995. Rel/NF-kappa B/I kappa B family: intimate tales of association and dissociation. Genes Dev. 9 (22), 2723–2735.

Vinothini, Kandasamy, Rajendran, Naresh Kumar, Ramu, Andy, Elumalai, Nandhakumar, Rajan, Mariappan, 2019. Folate receptor targeted delivery of paclitaxel to breast cancer cells via folic acid conjugated graphene oxide grafted methyl acrylate nanocarrier, Biomed. Pharmacother. 110, 906–917.

Vishtal, A., Kraslawski, A., 2011. Challenges in industrial applications of technical lignins. Bio Resources 6, 3547–3568.

Vogl, O., Tirrell, D., 1979. Functional polymers with biologically active groups. J. Macromol. Sci. Chem. 13, 415–439.

Wang, Z., Nakayama, T., 2010. Inflammation, a link between obesity and cardiovascular disease. Mediators Inflamm. 2010, 535918.

Welker, Cassie Marie, Balasubramanian, Vimal Kumar, Petti, Carloalberto, Rai, Krishan Mohan, DeBolt, Seth, Mendu, Venugopal, 2015. Engineering plant biomass lignin content and composition for biofuels and bioproducts. Energies 8, 7654–7676.

Xiao, Yunchao, Wang, Mengyuan, Lin, Lizhou, Du, Lianfang, Shen, Mingwu, Shi, Xiangyang, 2019. Specific capture and release of circulating tumor cells using a multifunctional nanofiber-integrated microfluidic chip. Nanomedicine (Lond.) 14, 183–199.

Yang, J., Lin, Y., Guo, Z., Cheng, J., Huang, J., Deng, L., Liao, W., Chen, Z., Liu, Z., Su, B., 2001. The essential role of MEKK3 in TNF-induced NF-kappaB activation. Nat. Immunol. 2 (7), 620–624.

Yang, B., Wyman, C.E., 2008. Pretreatment: The key to unlocking low-cost cellulosic ethanol. Biofuels Bioprod. Biorefin. 2, 26–40.

Yogeeswari, P., Sriram, D., 2005. Betulinic acid and its derivatives: a review on their biological properties. Curr Med Chem 12 (6), 657–666.

Yue, T.L., Mckenna, P.J., Gu, J.L., Feuerstein, G.Z., 1993. Interleukin-8 is chemotactic for vascular smooth muscle cells. Eur. J. Pharmacol. 240 (1), 81–84.

Zhang, D.M., Xu, H.G., Wang, L., Li, Y.J., Sun, P.H., Wu, X.M., Wang, G.J., Chen, W.M., Ye, W.C., 2015. Betulinic acid and its derivatives as potential antitumor agents. Med. Res. Rev. 35 (6), 1127–1155.